Advanced Fiber Materials (2023) 5:198–208
https://doi.org/10.1007/s42765-022-00208-w

RESEARCH ARTICLE

Highly Stretchable Ionic and Electronic Conductive Fabric

Pengfei Deng[1] · Xuan Li[1] · Yanbin Wang[1] · Zijian He[1] · Wenkai Zhu[1] · Yun Zhang[1] · Gabriella M. Schalm[1] · Tian Li[1]

Received: 4 June 2022 / Accepted: 4 September 2022 / Published online: 28 October 2022

Abstract

Wearable devices redefine the way people interact with machines. Despite the intensive effort in the design and fabrication of synthetic fibers to improve wearable device properties in terms of electronic and ionic conductivity, stretchability, comfort, and washability, challenges remain in fabricating single fiber materials that optimize all properties simultaneously. In this work, we demonstrate a highly stretchable, ionic, and electronic conductive fabric via (1) the natural nanoscale channels in fibers for effective ion transportation, (2) confining the electronic conductive material with the cellulose fibers, and (3) decoupling the property degradation of the fiber from deformation using the knitted pattern. The hierarchical structure created by cotton fibers can serve as ionic conductive channels as well as a robust multiscale scaffold to host infiltrated electronic conductive materials. Cotton strands with ionic and electronic conductivity can be knitted into fabrics that are highly stretchable (~300%). Moreover, high ionic and electronic conductivity are observed with 2 S/m and 5 S/m, respectively, even under a strain of 175%. With the inherent advantages of cotton fabrics such as moisture-wicking, washability, comfort, and light-weightiness for wearable applications, our approach of directly functionalized cellulose can potentially be a promising route towards highly stretchable and wearable mixed conductors.

Keywords Stretchability · Cellulose nanofibers · Mixed conductor · Topological pattern · Wearable devices

Introduction

With the fast evolvement of big data and intelligent technology, the need for sensing and collecting signals generated by human activities becomes critical. Thus, advanced wearable devices are developed for health monitoring [1, 2], intelligent sensing [3, 4], and human–machine interaction [5]. Wearable devices that effectively carry electronic signals even under mechanical deformations (e.g., stretching and twisting) have attracted tremendous attention [6]. To increase device stretchability, specific structures or patterns have been utilized for the intrinsically rigid semiconductors and metals that are widely used as electronic conductive materials [7–9]. Meanwhile, using soft matters as building blocks is another common strategy, because they have intrinsically lower tensile moduli that can potentially match the mechanical properties of biological tissues [10–12]. Although the high stretchability and electronic conductivity have been achieved via these two strategies, the lack of mixed conductivity especially in ionic domains has limited their applications in bioelectronics [13], energy storage [14], and functional organic transistor [15] as the next-generation wearable devices. Recently, polymer-based composite materials have been developed for mixed ionic-electronic conduction [16, 17]. Nevertheless, the synthetic polymer has difficulties in achieving high stretchability and conductivity simultaneously, the incompatibility between these two properties leads to poor electro-mechanical performance [18]. Also, the fabrication processes involving complex designs and high-level environmental control limit the possibility of large-scale production. Furthermore, most synthetic polymers lack air permeability and moisture-wicking capability when attached to human skin, making them less comfortable for daily human activities. Therefore, sustainable material that exhibits promising performance in high stretchability, mixed conductivity, and comfort is in urgent demand for next-generation wearable devices.

Cellulose is the most abundant biopolymer on Earth that can be massively extracted from the cell walls of wood, cotton, and other plants. Among all the types of cellulosic materials, cotton fibers have a long history

✉ Tian Li
tianli@purdue.edu

[1] School of Mechanical Engineering, Purdue University, West Lafayette 47907, USA

of being used by human beings due to their widespread usage in linen and apparel. Therefore, there is a potential to adopt this sustainable material for wearable device development. Cellulose, as the main component in cotton, features a naturally hierarchical structure down to the nanometer scale [19–21]. Cellulose fiber provides a scaffold with multiscale interspace and aligned nanochannels for ion transportation because the electrical double layer (EDL) is generated after the hydroxyl groups of cellulose molecules partially deprotonate under aqueous conditions (Fig. 1a). The hierarchical structure also contributes to the desired mechanical properties like flexibility. For example, the theoretical Young's modulus and tensile strength of the cellulose molecular (the lowest level on the nanometer scale) are 250 GPa and 7.5–7.7 GPa [22], respectively, while the experimental estimate for cotton fiber (in micrometer scale) has lower values of 5.5–13 GPa [23] and 0.3–1.4 GPa [24].

In this work, we directly functionalized natural cotton into ionic-electronic conductive fibers, which were then structured into a highly stretchable fabric via a topological pattern that is commonly adopted in textile knitting. We directly utilized the interspace among the numerous aligned nanofibril in cotton fibers as nanofluidic channels to conduct ions. And to effectively conduct electrons, Poly (3,4-ethylenedioxythiophene): poly (styrene sulfonate) (PEDOT: PSS) has been infiltrated into the interspace among single fibers (Fig. 1a). A general strategy to address the conflict between conductivity and stretchability is to preserve the morphology of the carrier transport channels upon stretching and twisting, where mixed conductivity and stretchability are decoupled. Therefore, a knitting pattern to create topologic configurations of cotton fibers were utilized, where the knitted 2D topological pattern offsets the tensile displacement under strains. As the actual length of pathways for ions and electrons is maintained under stretching, their transportations have been decoupled with strains, and high stretchability and mixed conductivity have been successfully preserved (Fig. 1b). Compared with the stretchability of cotton thread of only 12%, the stretchability of the fabrics has increased up to 300% which is four times of its initial length. The finite element analysis (FEA) confirms that the knitted pattern can effectively handle stretching by knitting structure displacement without the deformation of cotton threads. In addition, the interlocked junctions of threads in fabric naturally provide breathability, comfort, and durability. This topological designed rationale can also be applied to other one-dimensional linear materials to be two-dimensional with an enhancement of stretchability and compatible conductivity and stretchability. Compared with other materials like metals, synthetic polymer, and composite mixed conductors, our mixed conductive fabrics can potentially provide a route to meet the requirements for both wearability and ionic/electronic conductive devices via structural engineering and chemical modification (Fig. 1c).

Experimental Section

Materials

Poly(3,4-ethylenedioxythiophene): poly (styrene sulfonate) (PEDOT: PSS) (1.3 wt % dispersion in H_2O, conductive grade) and Dimethyl sulfoxides (DMSO) (Hybri-Max™, sterile-filtered, BioReagent, suitable for hybridoma, ≥ 99.7%) were obtained from Sigma-Aldrich.

Fabrication of the Mixed Conductive Fabric

Cotton fabric from a commercially available cloth was selected. First, the fabric was cut into several rectangular-shaped pieces. Then, the samples were transferred into a solution consisting of 95 wt.% PEDOT: PSS and 5 wt.% DMSO. All the mixture was placed in the sonication bath for 2 h at room temperature. Next, to fully infiltrate the PEDOT: PSS particles into the cellulose fabric scaffold, the mixture in vials was put into the vacuum pump, with a pressure of 25 Pa for 1 h. Finally, the fabric samples were picked up from vials and dried using a freeze-dryer or air-forced convection oven.

Morphology Characterizations

Scanning electron microscopy (SEM, Helios G4 UX dual-beam) was used to observe the morphology and the hierarchical structures of the fabrics. Small-angle X-ray Scattering (SAXS, Anton Paar SAXSpoint 2.0) was used to characterize the crystal structure and the orientation of cotton and nylon fibers.

Mechanical Tests

Tensile tests were conducted using ADMET Load Frame as a tensile meter to determine the stress–strain curves for single threads, twisted threads, plain-knitted fabrics, and double-knitted fabrics. The measured curves would reveal the overall performance of knitted fabrics under displacement, the ultimate strains and stress for each material.

Finite Element Analysis

Three-dimensional finite element analysis (FEA) was conducted via the commercial software ABAQUS to study the stress state in a 2 × 2 plain knitted fabric. Displacement defined by initial length and strains were applied as boundary conditions on the two sides of the models. The analysis

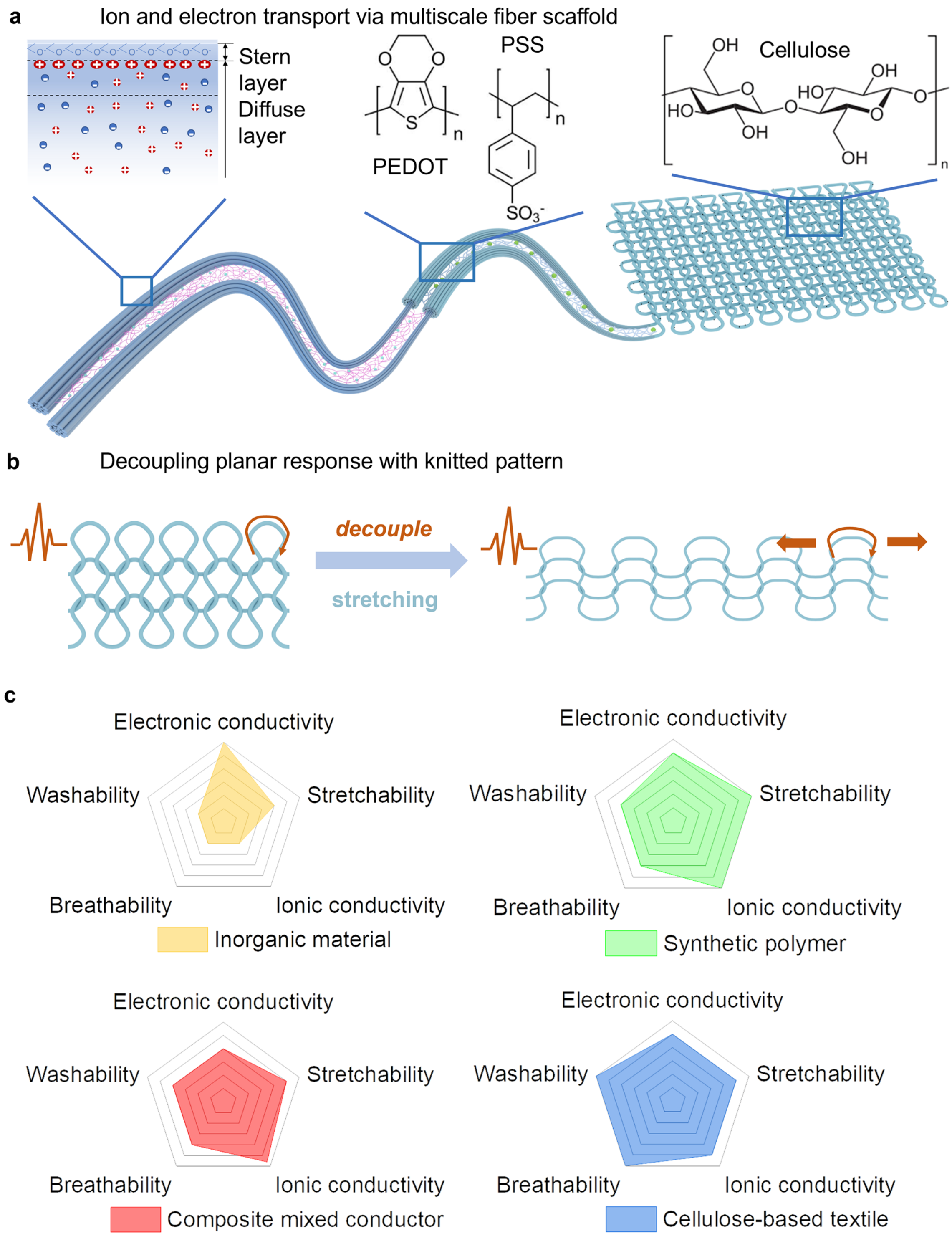

Fig. 1 Schematics of the Hierarchical Scaffold. **a** Schematic of the hierarchical structure of the mixed conductive fabric. **b** Mechanism of the topological pattern to enhance the stretchability. **c** Spider chart of our device with other reports (details in Supplementary Document S1)

was carried out for a single thread in the uniaxial direction, and for the fabrics in the biaxial direction. The maximum equivalent stress (von Mises stress) was used to determine the stress distribution.

Electrochemical Measurements

Electrochemical characteristics were tested on VSP Biologic electrochemical workstation. The electrochemical performance was measured with Ag/AgCl electrodes. The fabric was stretched by the stable moving stage (F100T2, Chemyx Inc). For every strain condition, electrochemical impedance spectroscopy (EIS) measurement was conducted with a frequency from 100 Hz to 1 MHz. The electronic conductivity was also measured by the Biologic electrochemical workstation, at which CV curves were swept from − 1 to 1 V.

Washability Experiments

Samples were stirred at 800 rpm in beakers to simulate the laundry in a washing machine. Each fabric has been prewashed for 0.5 h and then washed for 4 cycles with 0.5 h cycle time each. After each cycle, the sample was dried in a convection oven at 100 °C for 15 min. The mixed conductivity was tested following the same procedure described in Sect. 2.6.

Results and Discussion

Hierarchical Structure Characterizations

Characterizations of the morphology of cotton fibers were carried out to reveal the hierarchical structure. Scanning electron microscopy (SEM) images in Fig. 2a–e shows the hierarchical structure of the knitted fabric. Figure 2a shows the cross-section of a single cotton fiber which consists of numerous cellulose nanofibrils that are ~ 20 nm thick. The microfibrils (highlighted in Fig. 2b) are packaged into a larger unit, forming microfibril bundles, which are also called single fibers (Fig. 2c–e). The surface of a single fiber is composited of microfibrils with preferred local orientation (Fig. 2c). Figure 2c, d show a microfibril bundle with a twisted and tabular shape because the cellulose synthesized from plants contains a crystal form of cellulose Iβ, which has a monoclinic unit cell with the lattice parameters

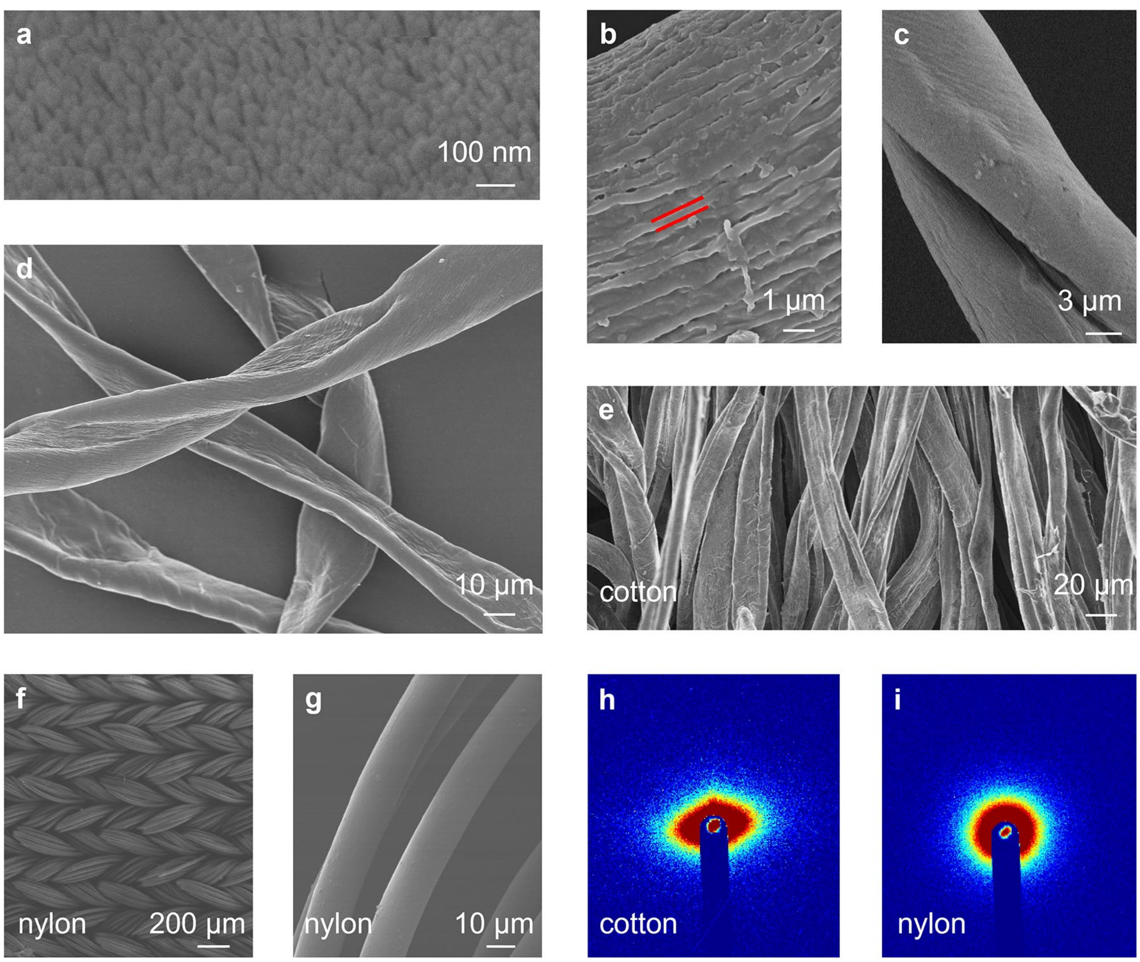

Fig. 2 Material characterization of the hierarchical structure of the cotton fibers. **a** SEM image of the cross-section of nanofibril. **b–d** SEM images of microfibril bundles. **e** SEM image of cotton thread. **f** SEM image of nylon fabric. **g** SEM image of nylon microfibrils. **h** SAXS image of cotton fabric. **i** SAXS image of nylon fabric

of $a = 7.784$ Å, $b = 8.201$ Å, $c = 10.380$ Å, $\alpha = 90°$, $\beta = 90°$, and $\gamma = 96.55°$ [25]. Shown in Fig. 2e are the numerous intertwined microscale fibers within a single cotton thread on a centimeter scale. As a comparison, the unique hierarchical structure commonly found in cellulose-based textile materials is hardly observed in synthetic garment fibers. For example, the microfibril of nylon has a smooth surface at the micrometer scale (Fig. 2f, g), while the microfibril bundle of cotton has a rough surface with multiscale morphology in a smaller size, and it can be further divided into micro-and nano-scale structures (Fig. 2a–e).

To explore the existence of nanofluidic channels that transports ions, a small-angle X-ray Scattering (SAXS) analysis was conducted, where interference patterns were characteristic of the internal structures of the materials including orientation and distances among atoms [26]. An elliptical pattern is observed for cotton fiber arising from the anisotropic scattering in different directions (Fig. 2h), which shows the orientation of the internal structure, verifying the alignment of the cotton fiber down to the nanoscale level. However, a circular pattern in the SAXS of nylon (Fig. 2i), where particles have identical shape and size, does not show the aligned nanoscale features-like cotton fibers. The hierarchical structure and locally aligned cellulose nanofibrils in cotton render the fabric as a scaffold with partially aligned inter-fiber space for allocating other active functional materials and facilitating nanofluid and ion transportation.

Solid Mechanics

Topological patterns created by knitting are usually utilized to enhance the stretchability of mixed ionic-electronic conductive fibers. Single cotton threads are typically soft and flexible but have limited stretchability, only 12% ultimate strain has been obtained from the tensile tests. When multiple single threads are twined in a spiral direction, a thicker thread can be produced with enhanced strength and stretchability (Fig. 3a, b). Ultimately, threads are often woven or knitted into certain patterns in fabric manufacture to further enhance mechanical properties [27, 28].

Consequently, theoretical modeling and finite element analysis (FEA) were conducted to investigate the contribution of topological patterns and pressure distribution on the fabrics and the mechanism of the stretching enhancement. We set up the topological modeling of the knitted pattern to find the ultimate strains in vertical and horizontal directions. The topological pattern alone will contribute to the strains of 80% and 142% in vertical and horizontal directions, respectively (Supplementary Document S2). Further increasing strains results from the intrinsic properties of fibers, where twisted thread-like properties have been found (Supplementary Document Fig. S1). According to FEA simulations, when uniaxial stress is applied, the stress is equally distributed in the fiber. However, in fabrics, the stress mainly emerges at the junctions, resulting in mostly stress-free fibers. When fibers and fabrics along different directions have been stretched to the strain of 20%, the ultimate stress in fiber reaches 130 MPa, but in fabrics, only 1.5 MPa and 1.0 MPa are shown in vertical (V) and horizontal (H) directions, respectively (Fig. 3c–e). Therefore, the topological knitted fabric pattern could prevent property degradation of cotton fibers by redistributing the applied load.

Tensile strength measurements were conducted to verify the hypothesis and design, and uniaxial loadings were applied to a single cotton thread, plain-knitted cotton fabric, and double-knitted cotton fabric (Fig. 3b, f–g). The stress–strain curves of plain-knitted fabrics are shown in Fig. 3f, the ultimate strain in the horizontal direction is 192%, nearly 3 times its original length. Besides, it is also shown that under tensile loadings, the cotton fibers in a thread are packed more densely, resulting in reduced void volume and higher Young's modulus with the increase of strains. The results also show that the double-knitted fabric can tolerate higher strain compared to plain-knitted cotton fabric in the horizontal direction and both have similar ultimate strains in the vertical direction (Fig. 3h). The fabrics fail at 192% and 365% strain in plain-knitted pattern and double knitted-pattern under the horizontal stretching but 120% and 117% strain under the vertical stretching. Both fabrics have remarkably increased ultimate strain and load compared to the single cotton thread that the fabrics are made of. Furthermore, the tensile tests of mixed fabrics coated with PEDOT: PSS have also been conducted to reveal its impact on overall mechanical properties. Although those coated with PEDOT: PSS has slightly reduced stretchability in both topological patterns (Fig. 3f–h), they still show promising stretchability for daily wear. The degradation comes from the infiltration and deposition of the PEDOT: PSS, by which the void spaces between fibers have been filled. Consequently, the mixed fabrics have a higher Young's modulus and become more brittle with the degraded stretchability.

The large stretchability difference along with two loading directions is hypothesized to come from the anisotropy of the knitting pattern of the fabric. The failure in the horizontal direction happens when single fibers reach their strength limit. By introducing a double-knitted pattern, a higher limit was observed for the fabric. For vertical stretching, failure happens when any one of the junctions breaks. The cotton fibers interact with the fibers under crosswise stretching, which easily breaks at junctions, leading to less ultimate strain. Mechanical analysis shows that fabric made from cotton thread has outstanding mechanical properties including flexibility and stretchability of the basis material under external stimulation. Note that other topological patterns could also be applied to other fiber materials to improve stretchability, and hyperplastic material can be incorporated

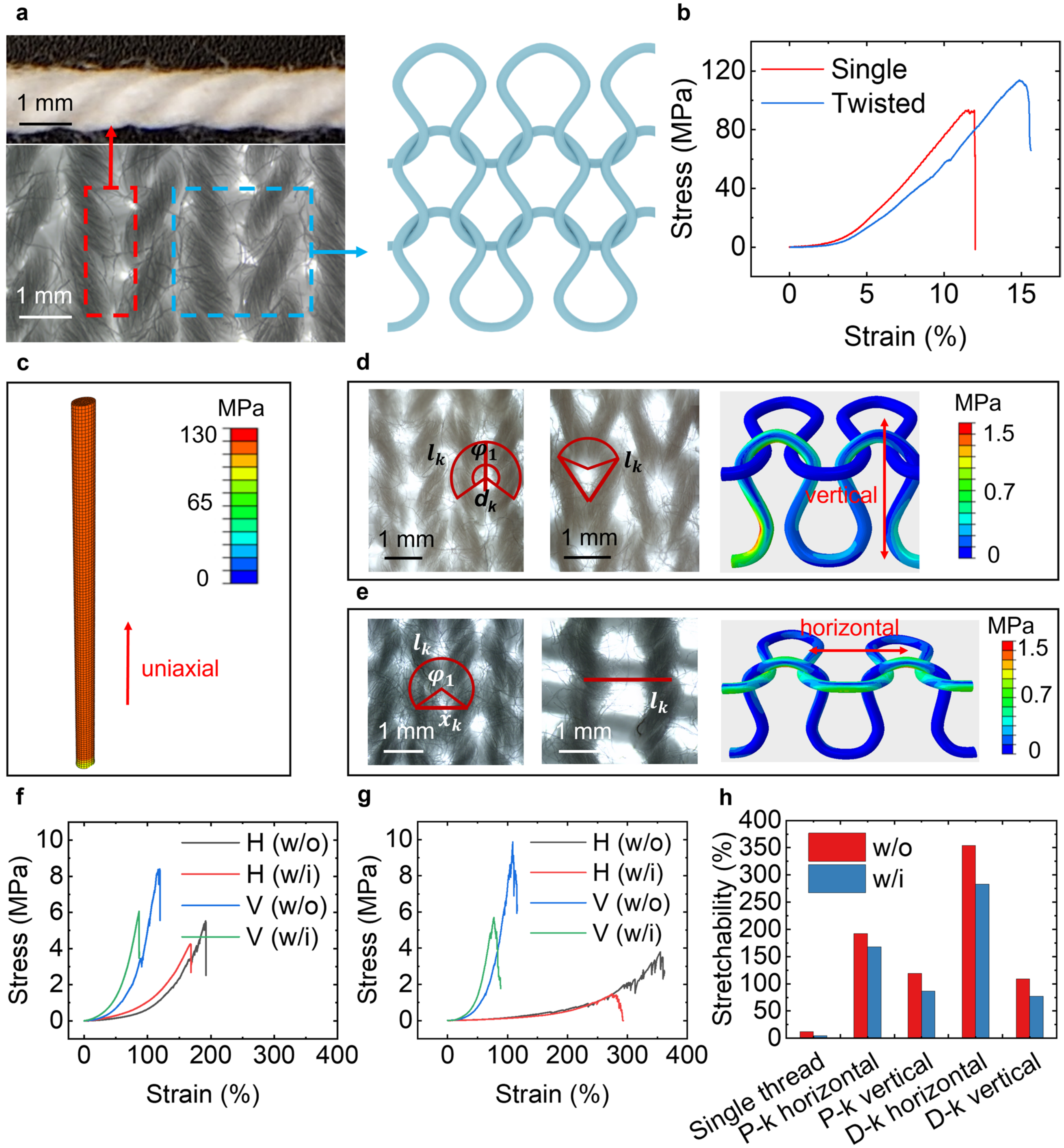

Fig. 3 Mechanical Analysis for Knitted Cotton Fabric. **a** Optical image of the twisted threads and schematic of plain knitted cotton fabric. **b** Stress–strain curves of single and twisted cotton thread. **c** FEA simulation result of single thread under axial stretch. **d** Optical microscopic images for theoretical modeling before (left) and after (middle) vertical stretch and FEA simulation result (right) of cotton fabric under vertical stretching. **e** Optical microscopic images for theoretical modeling before (left) and after (middle) horizontal stretch and FEA simulation result (right) of cotton fabric under horizontal stretching. **f** Stress–strain curves in horizontal (H) and vertical (V) directions of the plain-knitted cotton fabric with (w/i) and without (w/o) PEDOT: PSS coating. **g** Stress–strain curves in horizontal (H) and vertical (V) directions of the double-knitted cotton fabric with (w/i) and without (w/o) PEDOT: PSS coating **h** Stretchability (ultimate strains) of single threads, plain-knitted (P-k) and double-knitted (D-k) cotton fabric with (w/i) and without (w/o) PEDOT: PSS coating from the tensile tests

in the horizontal or vertical directions to reinforce stretchability accordingly.

Ionic/Electronic Mixed Conductivity

The hierarchically aligned cellulose fibers provide not only ions transport channels but also the multiscale scaffold to host other functional materials. With the multiscale channels, we demonstrate that the cotton fabric can be turned into an ionic and electronic mixed conductor by partially filling the voids with PEDOT: PSS, which will enhance the ionic conductivity and introduce the electrical conductivity of cotton fabrics. Figure 4a shows the mechanism of ionic and electrical conductivity of cotton fabric. Once PEDOT: PSS

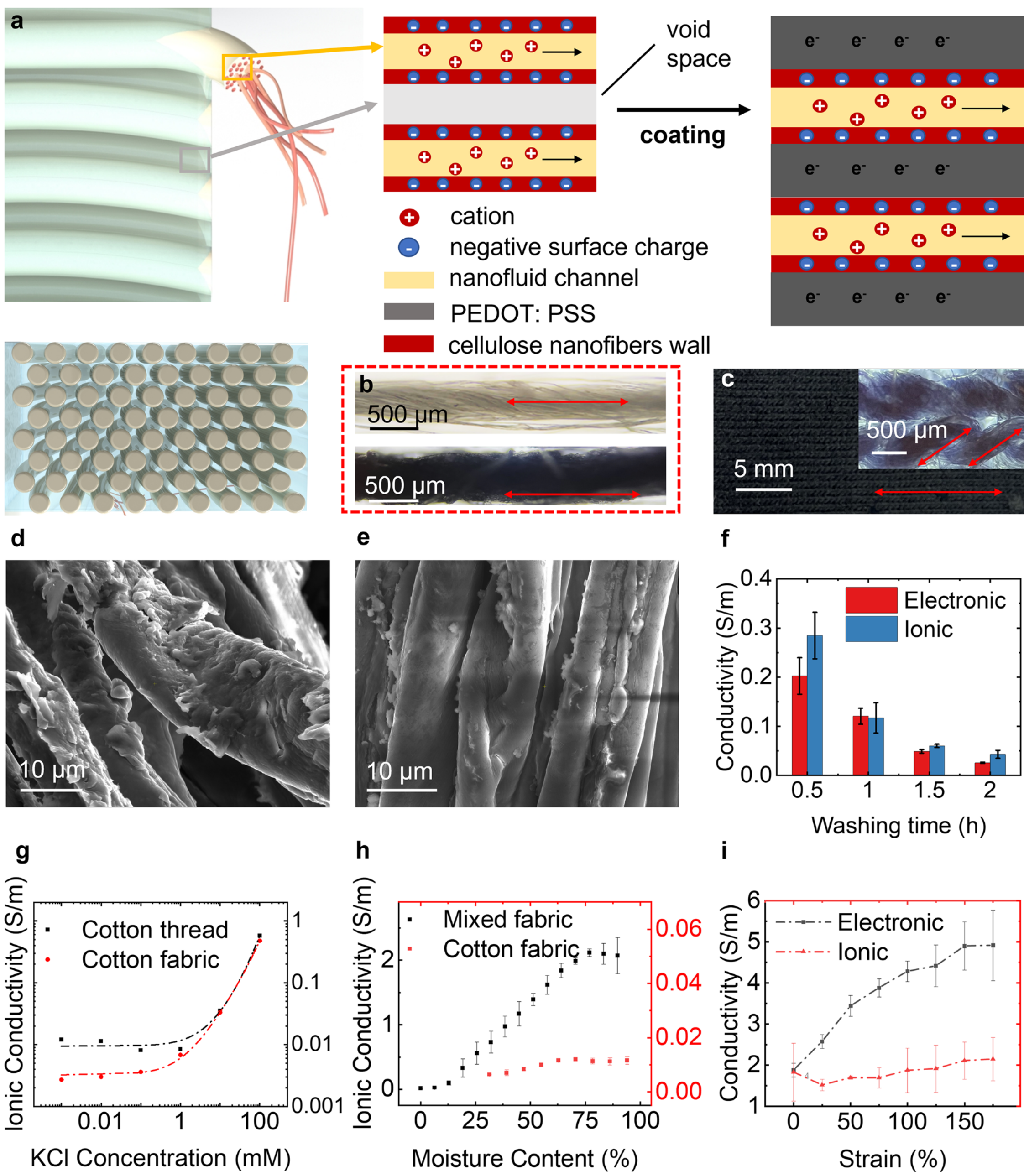

Fig. 4 The Ionic and Electrical Properties of Cotton Fabric. **a** Schematics of the mechanism of ionic and electrical conductivity of cotton fabric. **b** Optical microscope images of single tread coated without (upper) and with (lower) PEDOT: PSS. **c** Optical microscope images of PEDOT: PSS coated fabric with different scales. **d** SEM image of mixed fabrics before washing. **e** SEM image of mixed fabric after 2-h (4 cycles) washing. **f** Mixed ionic-electronic conductivity of fabric after washing cycles. **g** Ionic conductivity of cotton thread and cotton fabric in electrolyte (potassium chloride) solution with different concentrations. **h** Ionic conductivity of mixed fabric and cotton fabric under different moisture contents. **i** Mixed ionic-electronic conductivity of fabric under different strains

has been infiltrated into the void spaces and deposited on the fibers, it will serve as the pathway for electronic conduction, where holes would be provided by PEDOT-rich regions. When the composite fibers are under aqueous conditions, the hydroxyl group of cellulose will be partially deprotonated, leading to a negatively charged fiber surface and an electrostatic potential extending from the charged surface walls into the center of the channels. When the channels among cellulose fibers have a radius comparable to the characteristic length of the electrostatic potential (Debye length λ_d), the overlapped diffusing layers of the EDLs create the unipolar solution of counterions and electrostatically repel ions carrying charge with the same sign of the charged wall.

The optical images show the difference in light absorbance in the visible range after impregnating PEDOT: PSS into the cotton fabric (Fig. 4b, c). The SEM in Fig. 4d shows that the cotton fibers have been wrapped by PEDOT: PSS, serving as electronic conductive pathways. Due to the bonding between PEDOT: PSS and cellulose [29] as well as the protective twisting and turbulent cotton fiber shell (discussed in Sect. 3.1), PEDOT: PSS that is sheltered in microfibril bundle exhibits a desirable adhesion to the fiber scaffold even under washing for 2 h (Fig. 4e). The mixed ionic-electronic conductivity of the fabric has been tested as a demonstration of its washability. After the pre-washing process that washes away the conductive material which slightly adheres on the surface of fabrics, the fabric will have a decreased conductivity with cycling time. However, even after 2 h washing (4 cycles), the ionic and electronic conductivity keeps 0.05 S/m and 0.03 S/m, respectively (Fig. 4f). Consequently, together with the natural properties of cotton fabric, our fabric would be washable compared with the reported metals, synthetic polymers, and composite mixed conductors. The ionic conductivity of a single cotton thread is measured using potassium chloride (KCl) solution with different concentrations (Fig. 4g). A conductivity plateau was observed with the value of ~ 10^{-2} S/m when the solution concentration is below 1 mM, and the conductivity is ~ 0.57 S/m under 100 mM concentration of the solution. The plateau is commonly found in measuring the ionic conductivity of nanofluidic channels due to EDL overlapping and is a reveal of the nanofluid effect [30, 31]. Moreover, the results suggest that the ionic conduction at low concentrations is predominated by nanoscale transport, which is attributed to the enormous number of nanofluidic channels that exist in between nanofibrils.

Unlike commonly used nanofluidic materials including CNTs (1D structure) [32], graphene-based material (2D structure) [33, 34], polymeric porous particles (3D structure) [35], and anodic aluminum oxide (3D structure) [36], which is difficult to scale up high-performance fluidic channels due to orientations. Cellulose fibers feature a hierarchical structure with fluidic channel widths ranging from nanometers to millimeters and are inexpensive, renewable, and recyclable. Besides the nanofibrils defined channels, the PEDOT: PSS also contributes to the ionic conduction when it is sufficiently hydrated. PEDOT is hydrophobic and PSS is hydrophilic, as consequence, the as-cast PEDOT: PSS film has grains consisting of PEDOT-rich cores and PSS-rich shells. The grains accumulate in a pancake-like morphology surrounded by excess PSS. PSS completely dissociates into protons and PSS with a $pKa = 1.5$, so that cations can travel easily in the negatively charged PSS-rich domains, giving high ionic conduction [37]. Meanwhile, an Electrochemical Impedance Spectrum (EIS) was used to measure both ionic (frequency dependent) and electronic conductivity (frequency-independent) of mixed-conducting fabric. It's shown in Fig. 4h that the ionic conductivity of fabric before and after being coated with PEDOT: PSS are both dependent on moisture contents. Overall, the ionic conductivity rose with the increase of moisture content, resulting from the more actively mobile ions in aqueous environments. The ionic conductivity of the fabric increases 90 times with the integration of PEDOT: PSS.

Figure 4i shows the ionic and electronic conductivity under different strains. Moreover, due to the existence of the void between micro-channels, the conductive material could be bonded more tightly after stretching, leading to higher electronic conductivity. A higher electronic conductivity is observed after the fabric is stretched, possibly due to the elimination of vacancy between fibers and the increase in contacted area between PEDOT: PSS grains. On the other hand, the non-degradable ionic conductivity upon the increase of strains could result from the adhesion between PEDOT: PSS and cellulose scaffold, which provides continuous and aligned pathways for ion transportation.

Conclusion

This work demonstrates the development of a stretchable and wearable scaffold for mixed ionic and electronic conduction by adopting cellulose-based fabrics with a hierarchical structure. The hierarchical structure of cellulose-based fabric includes nanoscale fluidic channels defined by cellulose nanofibrils, microscale voids defined by single fibers, and millimeter-scale voids defined by knitted threads. The natural directional channels in cellulose nanofibrils facilitate effective ion transportation and provide a host for other active materials. With the enormous nanofluidic channels, the cotton fabric is an ideal scaffold for ions regulation. Moreover, the hydrophilic cellulose wall makes it easier to infuse aqueous ink like the PEDOT: PSS to form robust composite fibers which create a pathway for producing electronic conductive fabric. High conductivity is observed for both ionic and electronic conduction under 175% strain.

Such results prove the topological pattern can effectively decouple the property degradation from mechanical deformation since it occurs mostly in the topological pattern instead of in a single thread. Therefore, knitted cotton fabric is a promising candidate for wearable devices to achieve real-time health monitoring and energy harvesting due to its exceptional stretchability while maintaining its ionic and electronic conductivity.

Supplementary Information The online version contains supplementary material available at https://doi.org/10.1007/s42765-022-00208-w.

Acknowledgements The authors acknowledge Dr. Kejie Zhao and Xiaokang Wang for their helpful discussion.

We acknowledge the Start-up fund from Purdue University.

Declarations

Conflict of interest The authors have no conflict of interest to declare.

References

1. Li L, Liu Y, Song C, Sheng S, Yang L, Yan Z, Hu DJJ, Sun Q. Wearable alignment-free microfiber-based sensor chip for precise vital signs monitoring and cardiovascular assessment. *Adv Fiber Mater* **2022**;*4*:475.
2. Wang J, Wang L, Feng J, Tang C, Sun X, Peng H. Long-term In Vivo Monitoring of Chemicals with Fiber Sensors. *Adv Fiber Mater* **2021**;*3*:47.
3. Kang S, Zhao K, Yu D-G, Zheng X, Huang C. Advances in biosensing and environmental monitoring based on electrospun nanofibers. *Adv Fiber Mater* **2022**;*4*:404.
4. Wang W, Yu A, Zhai J, Wang ZL. Recent progress of functional fiber and textile triboelectric nanogenerators: towards electricity power generation and intelligent sensing. *Adv Fiber Mater* **2021**;*3*:394.
5. Cao R, Pu X, Du X, Yang W, Wang J, Guo H, Zhao S, Yuan Z, Zhang C, Li C, Wang ZL. Screen-printed washable electronic textiles as self-powered touch/gesture tribo-sensors for intelligent human-machine interaction. *ACS Nano* **2018**;*12*:5190.
6. Loke G, Alain J, Yan W, Khudiyev T, Noel G, Yuan R, Missakian A, Fink Y. Computing Fabrics. *Matter* **2020**;*2*:786.
7. Xue Z, Song H, Rogers JA, Zhang Y, Huang Y. Mechanically guided structural designs in stretchable inorganic electronics. *Adv Mater* **2020**;*32*:e1902254.
8. Fan JA, Yeo WH, Su Y, Hattori Y, Lee W, Jung SY, Zhang Y, Liu Z, Cheng H, Falgout L, Bajema M, Coleman T, Gregoire D, Larsen RJ, Huang Y, Rogers JA. Fractal design concepts for stretchable electronics. *Nat Commun* **2014**;*5*:3266.
9. Shyu TC, Damasceno PF, Dodd PM, Lamoureux A, Xu L, Shlian M, Shtein M, Glotzer SC, Kotov NA. A Kirigami approach to engineering elasticity in nanocomposites through patterned defects. *Nat Mater* **2015**;*14*:785.
10. Xu J, Wu HC, Zhu C, Ehrlich A, Shaw L, Nikolka M, Wang S, Molina-Lopez F, Gu X, Luo S, Zhou D, Kim YH, Wang GN, Gu K, Feig VR, Chen S, Kim Y, Katsumata T, Zheng YQ, Yan H, Chung JW, Lopez J, Murmann B, Bao Z. Multi-scale ordering in highly stretchable polymer semiconducting films. *Nat Mater* **2019**;*18*:594.
11. Oh JY, Rondeau-Gagne S, Chiu YC, Chortos A, Lissel F, Wang GN, Schroeder BC, Kurosawa T, Lopez J, Katsumata T, Xu J, Zhu C, Gu X, Bae WG, Kim Y, Jin L, Chung JW, Tok JB, Bao Z. Intrinsically stretchable and healable semiconducting polymer for organic transistors. *Nature* **2016**;*539*:411.
12. Wang GJN, Gasperini A, Bao Z. Stretchable polymer semiconductors for plastic electronics. *Adv Electron Mater* **2018**;*4*:1700429.
13. Ohayon D, Inal S. Organic bioelectronics: from functional materials to next-generation devices and power sources. *Adv Mater* **2020**;*32*:e2001439.
14. Zhu Y, Peng L, Fang Z, Yan C, Zhang X, Yu G. Structural engineering of 2D nanomaterials for energy storage and catalysis. *Adv Mater* **2018**;*30*:e1706347.
15. Inal S, Malliaras GG, Rivnay J. Benchmarking organic mixed conductors for transistors. *Nat Commun* **2017**;*8*:1767.
16. Han S, Alvi NUH, Granlof L, Granberg H, Berggren M, Fabiano S, Crispin X. A multiparameter pressure-temperature-humidity sensor based on mixed ionic-electronic cellulose aerogels. *Adv Sci (Weinh)* **2019**;*6*:128.
17. Tan STM, Gumyusenge A, Quill TJ, LeCroy GS, Bonacchini GE, Denti I, Salleo A. Mixed ionic-electronic conduction, a multifunctional property in organic conductors. *Adv Mater* **2022**;*34*:e2110406.
18. Lei Z, Wu P. A highly transparent and ultra-stretchable conductor with stable conductivity during large deformation. *Nat Commun* **2019**;*10*:3429.
19. Martin-Martinez FJ. Designing nanocellulose materials from the molecular scale. *Proc Natl Acad Sci USA* **2018**;*115*:7174.
20. Li T, Zhang X, Lacey SD, Mi R, Zhao X, Jiang F, Song J, Liu Z, Chen G, Dai J, Yao Y, Das S, Yang R, Briber RM, Hu L. Cellulose ionic conductors with high differential thermal voltage for low-grade heat harvesting. *Nat Mater* **2019**;*18*:608.
21. Zhang C, Chen M, Keten S, Coasne B, Derome D, Carmeliet J. Hygromechanical mechanisms of wood cell wall revealed by molecular modeling and mixture rule analysis. *Sci Adv* **2021**;*7*:1.
22. Moon RJ, Martini A, Nairn J, Simonsen J, Youngblood J. Cellulose nanomaterials review: structure, properties and nanocomposites. *Chem Soc Rev* **2011**;*40*:3941.
23. Varghese AM, Mittal V. Surface modification of natural fibers. In: Shimpi NG, editor. Biodegradable and biocompatible polymer composites. **2018**; pp. 115–186.
24. Han X, Ye Y, Lam F, Pu J, Jiang F. Hydrogen-bonding-induced assembly of aligned cellulose nanofibers into ultrastrong and tough bulk materials. *J Mater Chem A Mater* **2019**;*7*:27023.
25. Xie Y, Gao H, Zhang P, Qin C, Nie Y, Liu X. Preparation of degradable wood cellulose films using ionic liquids. *ACS Appl Polym Mater* **2022**;*4*:3598.
26. Putnam CD, Hammel M, Hura GL, Tainer JA. X-ray solution scattering (SAXS) combined with crystallography and computation: defining accurate macromolecular structures, conformations and assemblies in solution. *Q Rev Biophys* **2007**;*40*:191.
27. Fu K, Yang Z, Pei Y, Wang Y, Xu B, Wang Y, Yang B, Hu L. Designing textile architectures for high energy-efficiency human body sweat- and cooling-management. *Adv Fiber Mater* **2019**;*1*:61.
28. Liu X, Miao J, Fan Q, Zhang W, Zuo X, Tian M, Zhu S, Zhang X, Qu L. Recent progress on smart fiber and textile based wearable strain sensors: materials, fabrications and applications. *Adv Fiber Mater* **2022**;*4*:361.
29. Chen N, Luo B, Patil AC, Wang J, Gammad GGL, Yi Z, Liu X, Yen SC, Ramakrishna S, Thakor NV. Nanotunnels within poly(3,4-ethylenedioxythiophene)-carbon nanotube composite for highly sensitive neural interfacing. *ACS Nano* **2020**;*14*:8059.
30. Li T, Li SX, Kong W, Chen C, Hitz E, Jia C, et al. A nanofluidic ion regulation membrane with aligned cellulose nanofibers. *Sci Adv* **2019**;*5*:1.

31. Li T, Chen C, Brozena AH, Zhu JY, Xu L, Driemeier C, Dai J, Rojas OJ, Isogai A, Wagberg L, Hu L. Developing fibrillated cellulose as a sustainable technological material. *Nature* **2021**;*590*:47.
32. Ostler D, Kannam SK, Frascoli F, Daivis PJ, Todd BD. Efficiency of electropumping in nanochannels. *Nano Lett* **2020**;*20*:3396.
33. Liu M, Weston PJ, Hurt RH. Controlling nanochannel orientation and dimensions in graphene-based nanofluidic membranes. *Nat Commun* **2021**;*12*:507.
34. Min SK, Kim WY, Cho Y, Kim KS. Fast DNA sequencing with a graphene-based nanochannel device. *Nat Nanotechnol* **2011**;*6*:162.
35. Kobayashi Y, Honjo K, Kitagawa S, Uemura T. Preparation of porous polysaccharides templated by coordination polymer with three-dimensional nanochannels. *ACS Appl Mater Interfaces* **2017**;*9*:11373.
36. Zhu Z, Chen Y, Xu Z, Yu Z, Luo X, Zhou J, Tian Y, Jiang L. Super-spreading on superamphiphilic micro-organized nanochannel anodic aluminum oxide surfaces for heat dissipation. *iScience* **2021**;*24*:102334.
37. Rivnay J, Inal S, Salleo A, Owens RM, Berggren M, Malliaras GG. Organic electrochemical transistors. *Nat Rev Mater* **2018**;*3*:17086.

Pengfei Deng is now a graduate student in Mechanical Engineering at Purdue University. He received his bachelor's degree in Electrical Engineering at Huazhong University of Science and Technology. He is interested in renewable sustainable materials and devices. His research focuses on cellulose-based materials for wearable devices in different applications.

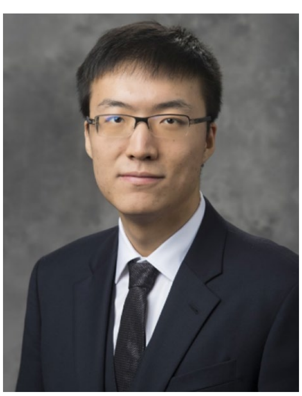

Xuan Li is now a PhD student in Agricultural and Biological Engineering at Purdue University. He received his Bachelor of Science in Mechanical Engineering from Purdue University. His current focus is on system automation for precision agriculture and plant phenotyping technologies.

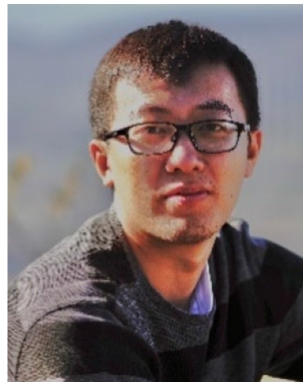

Yanbin Wang is now a postdoctoral fellow in Mechanical Engineering at Purdue University. He received his PhD at University of Maryland, College Park. His current research focuses on computational simulations, graph neural network, and drug delivery.

Zijian He is a master's student in Mechanical Engineering at Purdue University. He received his bachelor's degree in Mechanical Engineering at Purdue University.

Wenkai Zhu received his M.S./B.S. degree in Mechanical Engineering from Rensselaer Polytechnic Institute. He then pursued a Ph.D. degree in Mechanical Engineering at Purdue University. His research focuses on cellulose-based material innovation for energy transport applications including multiscale photonics and thermal management.

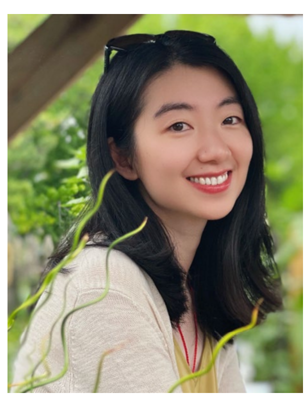

Yun Zhang received her Ph.D. degree in condensed matter physics and nanotechnology and her M.S. degree in Thermal Engineering from Xi'an Jiaotong University. She is currently a postdoctoral researcher in the Mechanical Engineering Department at Purdue University. Her current research focus is the heat and mass transport in sustainable materials and their interdisciplinary applications.

Gabriella Schalm is a 4th year undergraduate student in Mechanical Engineering at Purdue University and intends to graduate in May 2023. She is interested in mechanical design and sustainable technology, and studied at ESTACA in Paris, France for a semester in 2022.

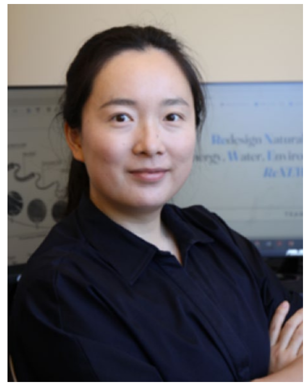

Tian Li is currently an Assistant Professor in School of Mechanical Engineering at Purdue University. She received her bachelor's degree from Huazhong University of Science and Technology in China. She obtained her PhD from the Department of Electrical and Computer Engineering at University of Maryland and carried out postdoctoral study in the Department of Materials Science and Engineering at the same university.